Supplementary Information

The Electro-catalytic Desalination with CO_2 Reduction and O_2 Evolution

Kaixiang Shen[1,2], Qiang Wei[1,2], Xin Wang[1,2], Qiang Ru[1], Xianhua Hou[1*], Guannan Wang[3*], Kwan San Hui[4], Jiadong Shen[5], Kwun Nam Hui[6*], and Fuming Chen[1,2*]

[1] Guangdong Provincial Key Laboratory of Quantum Engineering and Quantum Materials, School of Physics and Telecommunication Engineering, South China Normal University, Guangzhou 510006, P.R. China, Email: houxianhua@m.scnu.edu.cn; fmchen@m.scnu.edu.cn

[2] School of Electronic and Information Engineering, South China Normal University, Foshan, 528225

[3] College of Medical Engineering& the Key Laboratory for Medical Functional Nanomaterials, Jining Medical University, Jining, 272067, China. Email: chemwangguannan@gmail.com

[4] Engineering, Faculty of Science, University of East Anglia, Norwich, UK

[5] School of Materials Science, South China University of Technology, Guangzhou 510641, P.R. China.

[6] Joint Key Laboratory of the Ministry of Education, Institute of Applied Physics and Materials Engineering, University of Macau, Avenida da Universidade, Taipa, Macau, PR China. Email: bizhui@umac.mo

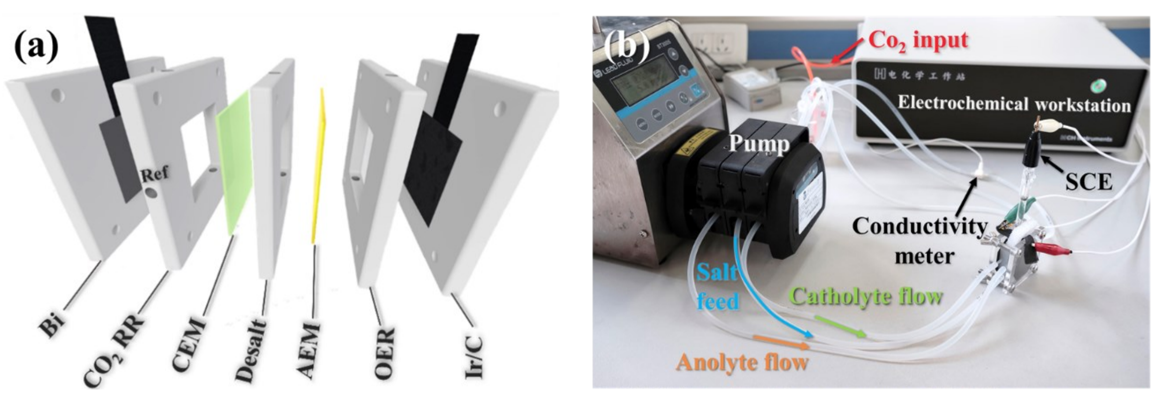

Figure S1. (a) The designed diagram of the multifunction electrocatalysis desalination device and (b) photo of electro-catalytic desalination setup.

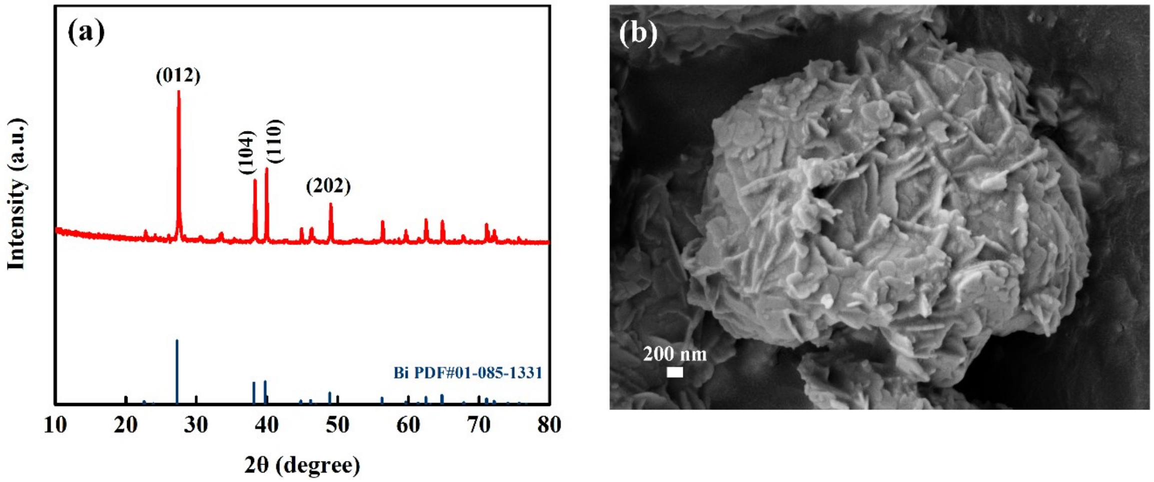

Figure S2. (a) XRD diffraction pattern of bismuth nano-powder, and (b) its SEM image

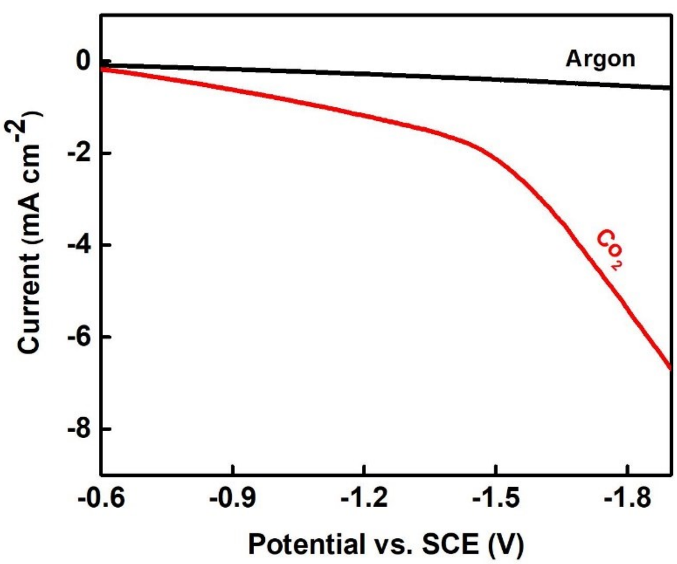

Figure S3. The LSV curves of Bi electrode in Argon and CO_2 saturated electrolyte. The typical three-electrode H-type cell is used with Pt counter and saturated calomel electrode (SCE) reference. The two reservoirs are separated by the cation exchanged membrane. Electrolyte: 0.5 M $NaHCO_3$; scan rate: 5 mVs^{-1}.

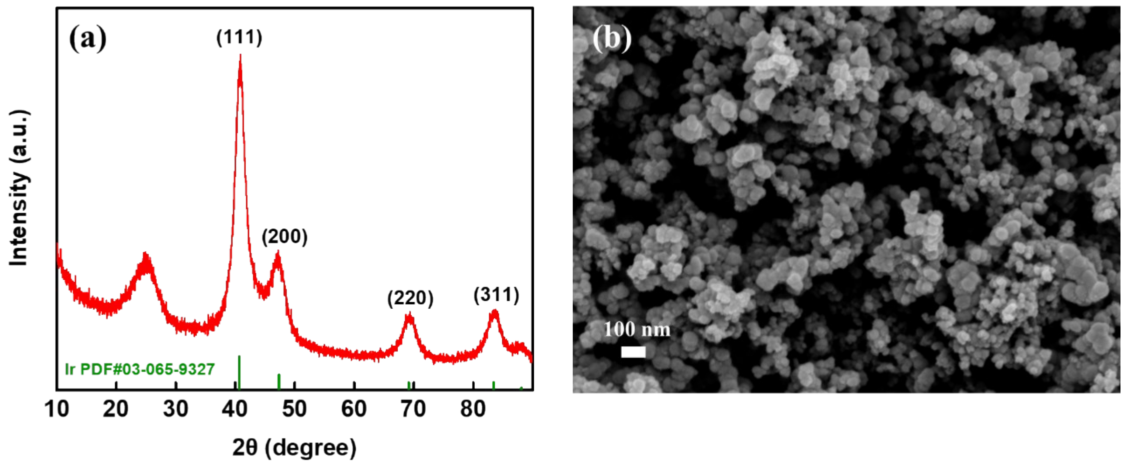

Figure S4. (a) XRD diffraction pattern of Ir/C nano-powder, and (b) its SEM image.

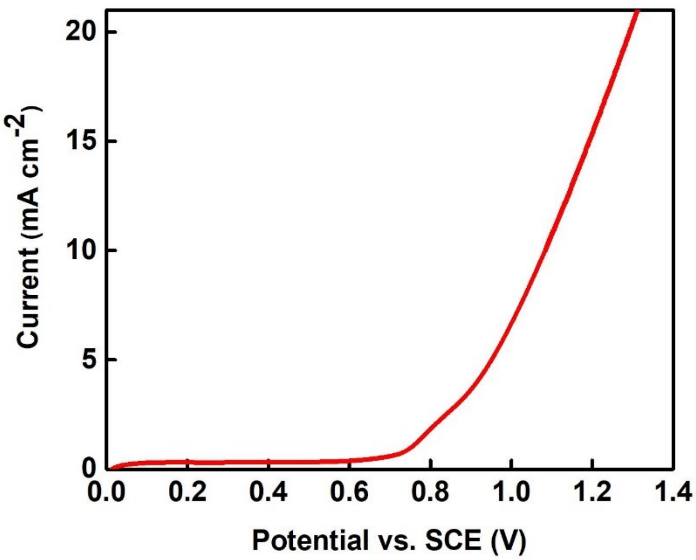

Figure S5. The LSV curve of Ir/C electrode in 0.5 M $NaHCO_3$, scan rate: 5 mVs^{-1}.

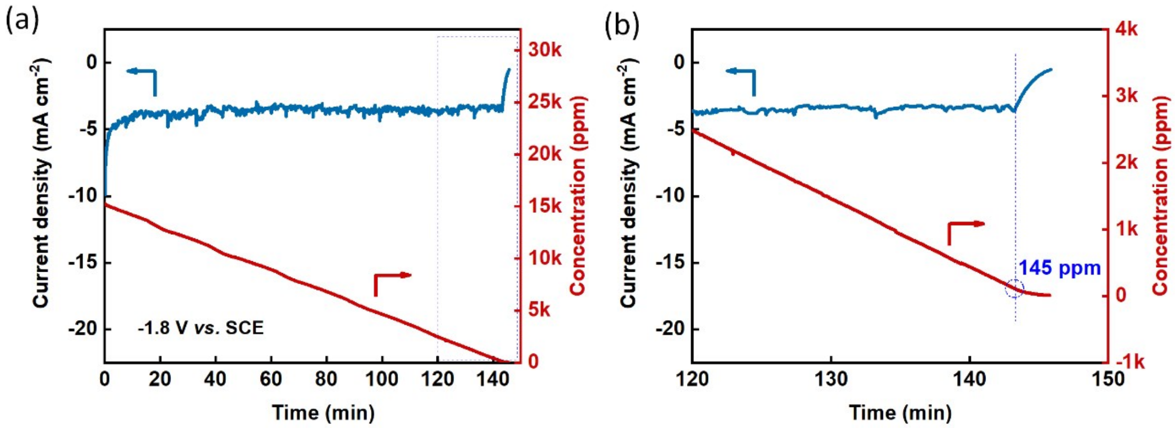

Figure S6. (a) The current density and continuous electrochemical performance of multi-function electrocatalysis desalination device at the constant potential of -1.8V applied. (b) The zoom-in sections at the last period in Figure S4a.

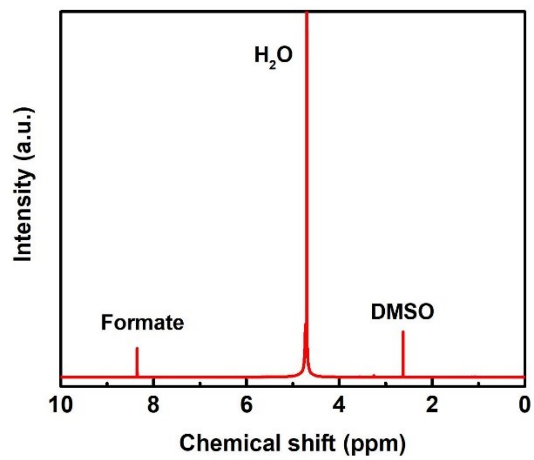

Figure S7. NMR spectra of the electrolyte in CO_2RR chamber after electrocatalytic desalination process, indicating formate generation.

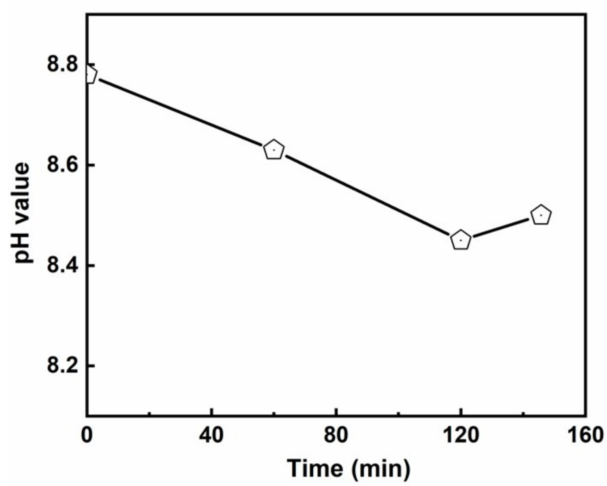

Figure S8. pH values in the OER chamber during the electrocatalytic desalination.

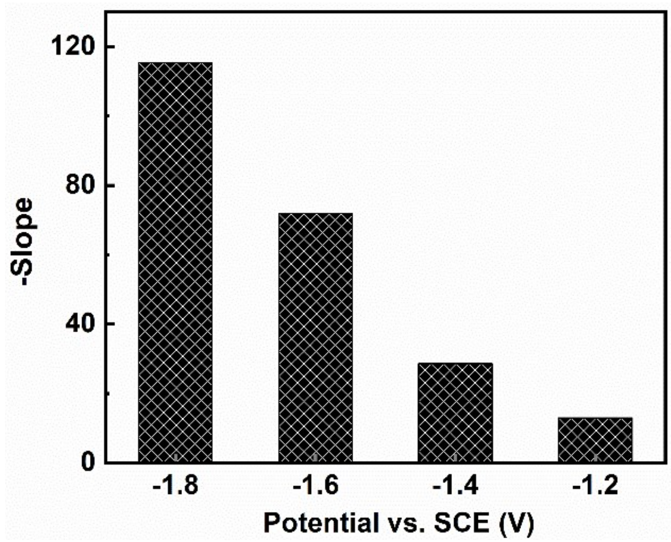

Figure S9. The relation between the potential and negative slope in Figure 2(a).

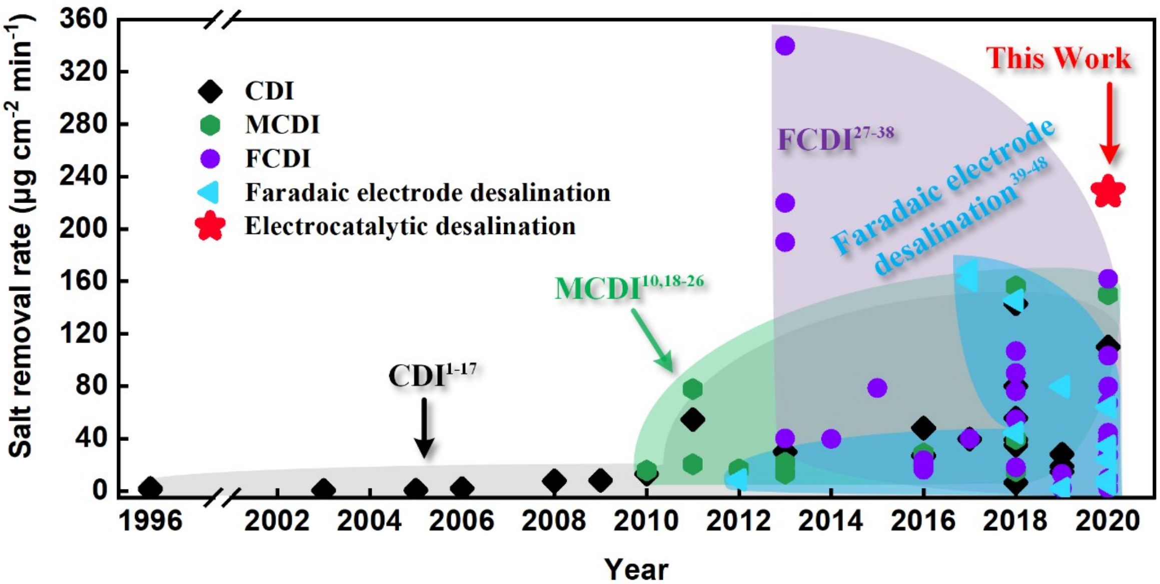

Figure S10. Historical evolution of salt removal rate for capacitive deionization (CDI)[1-17], membrane capacitive deionization (MCDI)[10, 18-26], flow-electrode capacitive deionization (FCDI)[27-37] and faradaic electrode desalination [38-47] as well as electrocatalytic desalination.

Table S1. The comparison of different desalination techniques: the electrode material, initial salt concentration, operation voltage/current, salt removal rate and energy consumption.

Desalination Technology	Electrode materials	Initial salt concentration (ppm)	Operation voltage/current	Salt removal rate (μg cm^{-2} min^{-1})	Energy Consumption# (kJ mol^{-1})	Year	Ref.
Capacitive deionization (CDI)	Carbon aerogel	~50 ~500	1.2 V	~0.99 ~2.05	-	1996	[1]
	Ti(1.05)/ACC	~5844	1.0 V	~0.35	-	2003	[2]
	MWCNTs	~3000	1.2 V	~0.45	-	2005	[3]
	CNTs-CNFs	~110	1.2 V	~1.97	-	2006	[4]
	Ordered mesoporous carbon	~25	1.2 V	~7.56	-	2008	[5]
	Ordered mesoporous carbon	~50	0.8 V	~8.09	-	2009	[6]
	Commercial Activated Carbon	~1169	1.2 V	~12.84	-	2010	[7]

	Phloroglucinol-based MC-coated graphite	35000	1.2 V	~ 54.54	-	2011	[8]
	MSP-20 (AC) OM SiC-CDC	~290	1.2 V	~29.79 ~26.67	-	2013	[9]
	AC-QPVP AC-HNO_3	500	1.0 V 1.2 V	~27.14 ~28.57	-	2016	[10]
	N-PHCS	500	1.2 V	~48	-	2016	[11]
	PTS-doped PAC	600	1.4 V	39.6	~0.24	2017	[12]
	GR/NMC	300	1.4 V	~55.56	-	2018	[13]
	S-AC || N-AC S-AC || AC N-AC || AC AC || AC	1000	1.4 V	~ 142.86 ~38.96 ~35.06 ~6.49	-	2018	[14]
	N, P, S co-doped hollow	500	1.2 V	80	-	2018	[15]

	carbon polyhedra						
	APTES groups onto activated carbon fabric	~1169	0.38 mA cm^{-2} 0.5 mA cm^{-2} 0.75 mA cm^{-2}	~14.64 ~18.73 ~28.10	~18 ~24 ~32	2019	[16]
	MOF/HG-2	800	1.4 V	~24.99	-	2020	[17]
Membrane capacitive deionization (MCDI)	activated carbon cloth	1000	1.2 V	-	~63	2006	[18]
	Porous carbon	~5260	1.4 V	~15.58	-	2010	[19]
	Carbon nanotubes	52	1.2 V	~20.41	-	2011	[20]
	Commercial activated carbon electrode	~292	1.2 V	~77.82	-	2011	[21]
	Porous carbon	~1169	1.2 V	~ 16.57	~110	2012	[22]
	Porous carbon electrodes	~1169	0.3 A 0.5 A 0.8 A	~13.32 ~21.52 ~26.63	-	2013	[23]

	Pristine AC electrodes	500	1.0 V 1.2 V	~20 ~28.57	-	2016	[10]
	Activated carbon	~1414	0.30 mA cm^{-2} 0.89 mA cm^{-2}	~15.11 ~39.70	~ 81.17 ~ 166.98	2018	[24]
	PCSs	~500	1.2 V	~156.25	-	2018	[25]
	SiW_{12}@PAN I/EGC	500	1.2 V	345 (after 10 mins) 150 (after 40 mins)	-	2020	[26]
Flow-electrode capacitive deionization (FCDI)	Carbon suspension	1100 5900 14200 32100	1.2 V	40 (~50% SRE[a]) 190 (~40% SRE) 220 (~20% SRE) 340(~12% SRE)	-	2013	[27]
	5% w/w dispersion of activated carbon powder	15000	1.2 V	~39.67	-	2014	[28]
	YP-50F activated carbon	10000	3.0 mA cm^{-2}	78.6	126.4	2015	[29]
	TE-3 activated carbon beads	1170	0.40 mA cm^{-2} 0.60 mA cm^{-2} 0.80 mA cm^{-2}	16.2 19.8	177.0 345.6	2016	[30]

			23.4	456.0		
Carbon suspension	35000	1.2 V	~39.85	-	2017	[31]
DARCO, and Noritactivated charcoal	2000	0.573 mA cm^{-2}	18	97.3	2018	[32]
		1.719 mA cm^{-2}	54.6	187.0		
		2.865 mA cm^{-2}	76.2	289.9		
		3.438 mA cm^{-2}	90	329.5		
		4.011 mA cm^{-2}	106.8	362.7		
AC + CB || CuHCF + CB	10000	1.4 V	13	-	2019	[33]
TEMPO	5860	0.06 mA cm^{-2}	1.986	78.2	2019	[34]
Activated carbon, carbon black, ferri-/ferrocyanide	9000	0.47 mA cm^{-2}	9.6	40.95	2020	[35]
		1.42 mA cm^{-2}	37.8	52.2		
		2.38mA cm^{-2}	78.6	98.07		
		3.33mA cm^{-2}	103.2	135.0		
		4.28 mA cm^{-2}	162	160.0		

	DARCO, and Noritactivated charcoal	1000	0.909 mA cm^{-2} 1.11 mA cm^{-2}	67.2 39.762	35.79 133.91	2020	36
	Carbon Black	1000	1.2 V	27.47 44.41	~125 ~122	2020	36
	50 mM/50 mM Ferri-/ferrocyanide	3000	0.06 mA cm^{-2} 1.11 mA cm^{-2}	1.90 39.76	1.57 133.91	2020	37
Faradaic electrode desalination	NMO||Ag	Seawater (~18500 Cl^-)	0.5 mA cm^{-2}	-	~151.3 (removal 25% Cl^-)	2012	38
	NMO||AgCl	~35000	1 mA	-	~0.04 kwh m^{-3}	2014	39
	BiOCl||NMO	~795	100 mA g^{-1}	160.71	96.88	2017	40
	AgCl||$Na_{0.44}MnO_2$	~ 891	100 mA g^{-1}	168.37	-	2017	41
	$FePO_4$@RGO||AC	~2500	100 mA g^{-1}	~145.45	~75.11	2018	42
	VCl_3||NaI	19000	0.22 mA cm^{-2}	~ 44.44	10.27	2018	43
	NVO@rGO||Ag@rGO	250	1.2 V	~1.70	-	2019	44

	NTP/rGO || AgNPs/rGO	2500	100 mA g^{-1}	~79.72	~26.89	2019	45
	Zn||Pt/C	3000	0.25 mA cm^{-2}	8.9	80.1(release)	2020	46
	Zn-$ZnCl_2$	2000	0.125 mA cm^{-2}	5	19	2020	47
			1.0 mA cm^{-2}	34	81.3		
			2.0 mA cm^{-2}	64	191.4		
Electrocatalytic desalination (ED)	Bi||n-TEC powered by PV cell	10000	peak at ~6 mA	-	~77.68[c]	2019	48
	Bi||n-TEC powered by DC	10000	peak at ~9.98 mA	-	~388.40[d]		
					~116.52[e]		
					~73.20[c]		
	Bi||Ir/C	15000	~ 3.6 mA cm^{-2} [f]	134.48	-	2021	This work
			~ 6.5 mA cm^{-2} [f]	228.41			
		12000	-1.2 V[b]	16.49	-		
			-1.4 V	36.53			
			-1.6 V	91.53			

[#] Energy consumption only includes the desalination devices without the consideration of pumps/equipment consumption.

[a] SRE: salt removal efficiency, the change in NaCl concentration is divided by the initial NaCl concentration.

[b] The voltage is relative to the saturated calomel electrode (SCE).

[c] The device is equipped with 5 desalination cell (DS) and desalinate to 50%.

[d] The device is equipped with 1 desalination cell and desalinate to 50%.

[e] The device is equipped with 3 desalination cell (DS) and desalinate to 50%

[f] At applied voltage of -1.8V *vs.* SCE, the current density can be offered stably.

References

1. J. C. Farmer, D. V. Fix, G. V. Mack, R. W. Pekala and J. F. Poco, *Journal of The Electrochemical Society*, 1996, **143**, 159-169.

2. M.-W. Ryoo and G. Seo, *Water Research*, 2003, **37**, 1527-1534.

3. K. Dai, L. Shi, J. Fang, D. Zhang and B. Yu, *Materials Letters*, 2005, **59**, 1989-1992.

4. X. Z. Wang, M. G. Li, Y. W. Chen, R. M. Cheng, S. M. Huang, L. K. Pan and Z. Sun, *Electrochemical and Solid-State Letters*, 2006, **9**, E23.

5. L. Zou, L. Li, H. Song and G. Morris, *Water Research*, 2008, **42**, 2340-2348.

6. L. Li, L. Zou, H. Song and G. Morris, *Carbon*, 2009, **47**, 775-781.

7. R. Zhao, P. M. Biesheuvel, H. Miedema, H. Bruning and A. van der Wal, *The Journal of Physical Chemistry Letters*, 2010, **1**, 205-210.

8. C. Tsouris, R. Mayes, J. Kiggans, K. Sharma, S. Yiacoumi, D. DePaoli and S. Dai, *Environmental Science & Technology*, 2011, **45**, 10243-10249.

9. S. Porada, L. Borchardt, M. Oschatz, M. Bryjak, J. S. Atchison, K. J. Keesman, S. Kaskel, P. M. Biesheuvel and V. Presser, *Energy & Environmental Science*, 2013, **6**, 3700-3712.

10. T. Wu, G. Wang, F. Zhan, Q. Dong, Q. Ren, J. Wang and J. Qiu, *Water Research*, 2016, **93**, 30-37.

11. S. Zhao, T. Yan, H. Wang, G. Chen, L. Huang, J. Zhang, L. Shi and D. Zhang, *Applied Surface Science*, 2016, **369**, 460-469.

12. R. L. Zornitta, F. J. García-Mateos, J. J. Lado, J. Rodríguez-Mirasol, T. Cordero, P. Hammer and L. A. M. Ruotolo, *Carbon*, 2017, **123**, 318-333.

13. T. Yan, J. Liu, H. Lei, L. Shi, Z. An, H. S. Park and D. Zhang, *Environmental Science: Nano*, 2018, **5**, 2722-2730.

14. T. Yan, B. Xu, J. Zhang, L. Shi and D. Zhang, *RSC Advances*, 2018, **8**, 2490-2497.

15. J. Zhang, J. Fang, J. Han, T. Yan, L. Shi and D. Zhang, *Journal of Materials Chemistry A*, 2018, **6**, 15245-15252.

16. A. C. Arulrajan, D. L. Ramasamy, M. Sillanpää, A. van der Wal, P. M. Biesheuvel, S. Porada and J. E. Dykstra, *Advanced Materials*, 2019, **31**, 1806937.

17. J. Feng, L. Liu and Q. Meng, *Journal of Colloid and Interface Science*, 2021, **582**, 447-458.

18. J.-B. Lee, K.-K. Park, H.-M. Eum and C.-W. Lee, *Desalination*, 2006, **196**, 125-134.

19. P. M. Biesheuvel and A. van der Wal, *Journal of Membrane Science*, 2010, **346**, 256-262.

20. H. Li and L. Zou, *Desalination*, 2011, **275**, 62-66.

21. P. M. Biesheuvel, R. Zhao, S. Porada and A. van der Wal, *Journal of Colloid and Interface Science*, 2011, **360**, 239-248.

22. R. Zhao, P. M. Biesheuvel and A. van der Wal, *Energy & Environmental Science*, 2012, **5**, 9520-9527.

23. R. Zhao, O. Satpradit, H. H. M. Rijnaarts, P. M. Biesheuvel and A. van der Wal, *Water Research*, 2013, **47**, 1941-1952.

24. L. Wang and S. Lin, *Water Research*, 2018, **129**, 394-401.

25. Y. Li, X. Xu, S. Hou, J. Ma, T. Lu, J. Wang, Y. Yao and L. Pan, *Chemical Communications*, 2018, **54**, 14009-14012.

26. H. Liu, J. Zhang, X. Xu and Q. Wang, *Chemistry – A European Journal*, 2020, **26**, 4403-4409.

27. S.-i. Jeon, H.-r. Park, J.-g. Yeo, S. Yang, C. H. Cho, M. H. Han and D. K. Kim, *Energy & Environmental Science*, 2013, **6**, 1471-1475.

28. Y. Gendel, A. K. E. Rommerskirchen, O. David and M. Wessling, *Electrochemistry Communications*, 2014, **46**, 152-156.

29. K. B. Hatzell, M. C. Hatzell, K. M. Cook, M. Boota, G. M. Housel, A. McBride, E. C. Kumbur and Y. Gogotsi, *Environ Sci Technol*, 2015, **49**, 3040-3047.

30. G. J. Doornbusch, J. E. Dykstra, P. M. Biesheuvel and M. E. Suss, *Journal of Materials Chemistry A*, 2016, **4**, 3642-3647.

31. Y. Cho, K. S. Lee, S. Yang, J. Choi, H.-r. Park and D. K. Kim, *Energy & Environmental Science*, 2017, **10**, 1746-1750.

32. C. He, J. Ma, C. Zhang, J. Song and T. D. Waite, *Environmental Science & Technology*, 2018, **52**, 9350-9360.

33. J. Chang, F. Duan, H. Cao, K. Tang, C. Su and Y. Li, *Desalination*, 2019, **468**, 114080.

34. J. Wang, Q. Zhang, F. Chen, X. Hou, Z. Tang, Y. Shi, P. Liang, D. Y. W. Yu, Q. He and L.-J. Li, *Journal of Materials Chemistry A*, 2019, **7**, 13941-13947.

35. Q. Wei, Y. Hu, J. Wang, Q. Ru, X. Hou, L. Zhao, D. Y. W. Yu, K. San Hui, D. Yan, K. N. Hui and F. Chen, *Carbon*, 2020, **170**, 487-492.

36. J. Ma, C. Zhang, F. Yang, X. Zhang, M. E. Suss, X. Huang and P. Liang, *Environmental Science & Technology*, 2020, **54**, 1177-1185.

37. F. Chen, J. Wang, C. Feng, J. Ma and T. David Waite, *Chemical Engineering Journal*, 2020, **401**, 126111.

38. M. Pasta, C. D. Wessells, Y. Cui and F. La Mantia, *Nano Letters*, 2012, **12**, 839-843.

39. M. Ye, M. Pasta, X. Xie, Y. Cui and C. S. Criddle, *Energy & Environmental Science*, 2014, **7**, 2295-2300.

40. F. Chen, Y. Huang, L. Guo, L. Sun, Y. Wang and H. Y. Yang, *Energy & Environmental Science*, 2017, **10**, 2081-2089.

41. F. Chen, Y. Huang, L. Guo, M. Ding and H. Y. Yang, *Nanoscale*, 2017, **9**, 10101-10108.

42. L. Guo, Y. Huang, M. Ding, Z. Y. Leong, S. Vafakhah and H. Y. Yang, *Journal of Materials Chemistry A*, 2018, **6**, 8901-8908.

43. X. Hou, Q. Liang, X. Hu, Y. Zhou, Q. Ru, F. Chen and S. Hu, *Nanoscale*, 2018, **10**, 12308-12314.

44. Z. Yue, Y. Ma, J. Zhang and H. Li, *Journal of Materials Chemistry A*, 2019, **7**, 16892-16901.

45. Y. Huang, F. Chen, L. Guo, J. Zhang, T. Chen and H. Y. Yang, *Desalination*, 2019, **451**, 241-247.

46. J. Dai, N. L. Win Pyae, F. Chen, M. Liang, S. Wang, K. Ramalingam, S. Zhai, C.-Y. Su, Y. Shi, S. C. Tan, L. Zhang and Y. Chen, *ACS Applied Materials & Interfaces*, 2020, **12**, 25728-25735.

47. J. Dai, J. Wang, X. Hou, Q. Ru, Q. He, P. Srimuk, V. Presser and F. Chen, *ChemSusChem*, 2020, **13**, 2792-2798.

48. B.-j. Kim, G. Piao, S. Kim, S. Y. Yang, Y. Park, D. S. Han, H. K. Shon, M. R. Hoffmann and H. Park, *ACS Sustainable Chemistry & Engineering*, 2019, **7**, 15320-15328.